Jurnal Sains Nuklear Malaysia, 2026, 38(Special Issue): 53 – 61
ISSN: 2232-0946

SYNTHESIS AND CHARACTERIZATION OF CERIUM OXIDE NANOPARTICLES VIA PRECIPITATION–CALCINATION METHOD

Cik Rohaida Che Hak[1*] and Siti Aisyah Aqilah Mohd Azny[2]

[1]Industrial Technology Division, Agensi Nuklear Malaysia, Bangi,
43000 Kajang, Selangor, Malaysia.
[2]Faculty of Applied Science, Universiti Teknologi MARA, Cawangan Perlis, Arau, Perlis
*Correspondence author: rohaida@nm.gov.my

ABSTRACT

Cerium is classified as a rare earth element suitable in many industrial applications. Cerium oxide (CeO_2), in particular has been widely used as catalysts in the petrochemical industries. Recently, CeO_2 has been investigated for its potential in sensor technology application, especially in biosensing. In this study, nanoporous CeO_2 was successfully synthesized through a precipitation -calcination route using cerium (IV) sulfate hydrate as a precursor. The synthesis involved pH-controlled precipitation at room temperature using ammonium hydroxide as the precipitation agent. The solid precipitate was separated from the excess liquid and dried overnight in an oven. The precipitate was then calcined at 600°C for 2 hours. Structural and morphological characterization was performed using Fourier Transform Infrared Spectroscopy (FTIR) and Field Emission Scanning Electron Microscopy (FESEM). FTIR analysis confirmed that the synthesis converted the hydroxide-sulfate precursor to CeO_2, as evidenced by the disappearance of sulfate bands and the emergence of Ce-O lattice vibrations. FESEM imaging revealed a nanoporous morphology with uniform particle distribution. Elemental compositional analysis via Energy Dispersive X-ray Spectroscopy (EDX) confirmed the presence of Ce with minimal residual sulfur contamination, while X-Ray diffraction (XRD) analysis exhibited the formation of CeO_2 phase. The synthesis yielded an 85% mass retention, demonstrating the potential of this route for efficient production of high-purity CeO_2.

Keywords: cerium oxide, nanoparticles, precipitation-calcination, thermal decomposition

Abstrak

Cerium dikelaskan sebagai sejenis unsur nadir bumi yang sesuai untuk pelbagai aplikasi industri. Khususnya, cerium oksida (CeO_2) telah digunakan secara meluas sebagai pemangkin di dalam industri petrokimia. Terkin CeO_2 telah dikaji akan potensinya dalam aplikasi teknologi penderiaan, terutamanya dalam penderiaan bio. Dalam kajian ini, CeO_2 berliang nano telah berjaya disintesis melalui laluan pemendakan-pengkalsinan dengan menggunakan cerium (IV) sulfat terhidrat sebagai bahan pemula. Sintesis ini melibatkan pemendakan terkawal pH pada suhu bilik menggunakan ammonium hidroksida sebagai ejen pemendakan. Mendakan pepejal tersebut dipisahkan daripada lebihan cecair dan dikeringkan semalaman di dalam ketuhar. Mendakan itu kemudiannya dikalsinkan pada suhu 600°C selama 2 jam. Pencirian struktur dan morfologi telah dijalankan menggunakan Spektroskopi Inframerah Transformasi Fourier (FTIR) dan Mikroskop Elektron Imbasan Pancaran Medan (FESEM). Analisis FTIR mengesahkan bahawa sintesis tersebut telah menukarkan bahan pemula hidroksida-sulfat kepada CeO_2, seperti yang dibuktikan melalui kehilangan jalur sulfat dan kemunculan getaran kekisi Ce-O. Imej FESEM mendedahkan morfologi berliang nano dengan taburan zarah yang seragam. Analisis komposisi unsur melalui Spektroskopi Sinar-X Serakan

Tenaga (EDX) mengesahkan kehadiran Ce dengan pencemaran sisa sulfur yang minimum, manakala analisis Belauan Sinar-X (XRD) menunjukkan pembentukan fasa CeO_2. Sintesis ini menghasilkan pengekalan jisim sebanyak 85%, menunjukkan kecekapan laluan ini berpotensi untuk menghasilkan CeO_2 dengan ketulenan tinggi.

INTRODUCTION

In the last several years, Ce-based compounds have received attention because of their widespread applications in industrial applications (Dahle & Arai, 2015). Cerium's unique electronic configuration specifically the 4f electrons shielded by 5s and 5p orbitals, contributes to its chemical versatility and enables variable valence reactions (Campbell & Peden, 2005). In addition, the ability of cerium to transition between Ce^{3+} and Ce^{4+}oxidation states generates oxygen vacancies that facilitate various catalytic processes (Campbell & Peden, 2005). Cerium oxide (CeO_2) particularly, has been extensively studied for its role in oxidation-reduction reactions, making it a critical material in automotive catalytic converters and solid oxide fuel cells (Sun et al., 2012). Recent advancements in nanotechnology have further enhanced the interest in CeO_2 nanoparticles for biomedical use, owing to their "nanozyme" activities, including peroxidase-, superoxide dismutase-, and catalase-like reactions (Das et al., 2013, Zhan et al., 2012, Mahmoud et al., 2022). These properties make CeO_2 nanoparticles (NPs) excellent candidates for biosensing applications, offering dual-mode detection capabilities with sub-picogram sensitivity (Wang et al., 2024).

Cerium (Ce) is one of the rare earth elements (REEs) belonging to the lanthanide series, and is the most abundant rare earth element in the Earth's crust It is commonly found in minerals such as monazite and bastnäsite (Gupta&Krishnamurthy, 2005). In addition to Ce, Malaysian monazite contains several other rare earth elements, including Lanthanum (La), Neodymium (Nd), Praseodymium (Pr), Samarium (Sm), and others. Monazite is also contaminated with thorium, a naturally occurring radioactive material, which raises radiological concerns and limits its applications. Furthermore, the extraction of CeO_2 from monazite involves multiple processing steps, including acid digestion, extensive separation of cerium from other rare earth elements, and complex solvent extraction procedures for purification. These processes are time-consuming and may take several weeks to months to complete.

Owing to these limitation, this study investigates the potential of synthesis CeO_2 NPs via a simple precipitation-calcination method. Various synthesis routes for CeO_2 NPs have been reported, including chemical precipitation-calcination (Pouretedal & Kadkhodaie, 2010), sol-gel (Alifanti et al., 2003), thermal decomposition (Wang et al., 2002), hydrothermal (Phoka et al., 2012), and combustion method (Bojana et al., 2008). Among these approaches, precipitation-calcination remains the predominant method due to its simplicity, scalability, and cost-effectiveness (Dahle & Arai, 2015). In this study cerium (IV) sulfate hydrate has been chosen as the precursor, owing to its high solubility, well-defined hydration states, and predictable thermal decomposition pathway. A straightforward synthesis route for CeO_2 NPs was developed through controlled precipitation followed by calcination. The structural evolution from precursor to final oxide and the morphological characteristics of the resulting NPs were characterized using FTIR spectroscopy and electron microscopy. The formation of CeO_2 after calcination was confirmed using X-ray diffraction (XRD).

MATERIALS AND METHODS

Materials

Cerium(IV) sulfate hydrate ($Ce(SO_4)_2 \cdot xH_2O$), ammonium hydroxide (25% NH_4OH), and distilled water were used as received without further purification. All chemicals were of analytical grade.

Synthesis Procedure

The synthesis was carried out following a modified chemical precipitation-calcination method (Krystof & Ondrejl, 2019). Cerium(IV) sulfate hydrate (3.25 g) was dissolved in 5 mL of distilled water under vigorous magnetic stirring until complete dissolution. Ammonium hydroxide solution (25%) was added dropwise under continuous pH monitoring until precipitation occurred The resulting precipitate was separated by vacuum filtration and washed repeatedly with distilled water to remove residual ammonium sulfate and unreacted ions. The collected material was dried overnight at 80°C in a convection oven and subsequently ground to a fine powder using a mortar and pestle. Calcination was performed in an alumina crucible using a programmable muffle furnace with a heating rate of 30°C/min to 600°C, maintained for 2 hours, and then allowed to cool naturally to room temperature.

Characterization

Fourier Transform Infrared (FTIR) spectroscopy was performed using a benchtop Cary 630 FTIR by Agilent to monitor the chemical transformation from precursor to oxide and to confirm the removal of sulfate groups. Field Emission Scanning Electron Microscopy (FE-SEM) of GeminiSEM-500 by Carl Zeiss coupled with Energy Dispersive X-ray Spectroscopy (EDS) of XMax-80 by Oxford Instruments was used to examine particle morphology, size distribution, and elemental composition. Samples for FESEM analysis were prepared by mounting powder on carbon-coated stubs, followed by sputter-coating with a thin conductive layer to prevent charging. X-Ray Diffraction (XRD) was employed to confirm the formation of CeO_2 and to evaluate its crystallinity used to determine the CeO_2 formation and its crystallinity.

RESULTS AND DISCUSSIONS

Formation of cerium oxide powder

Figure 1 shows the physical appearance of the cerium compounds before and after calcination, synthesized via the sonication-assisted precipitation of cerium hydroxide-sulfate. A distinct colour change is observed, from dark yellow in the precipitate to pale yellow in the post-calcination powder.

(a) (b) (c)

Figure 1: Cerium compounds; a) Precipitated cerium sulfate hydroxide after sonication; b) dried precipitate cerium sulfate hydroxide before calcining; c) post calcination powder.

FTIR Analysis

FTIR spectroscopy was employed to characterize the cerium(IV) sulfate hydrate, and the precipitated cerium hydroxide-sulfate both before and after calcination by identifying the chemical bonds and functional groups present. The FTIR spectra of the three samples are shown in Figure 2. A broad band centered around 3398 cm^{-1} was attributed to the O-H stretching vibrations of both adsorbed water and surface hydroxyl groups present in all samples. Another band around 1640 cm^{-1} related to the H-O-H bending mode were also observed in all samples. The stretching band is particularly broad due to the complex interactions between water molecules via hydrogen bonds.

The sulfate ion ($SO4^{2-}$) exhibits several characteristic infrared (IR) absorption bands associated with its vibrational modes. The consistent absorption observed around 1300-1400 cm^{-1} across all samples is attributed to sulfate (SO_4^{2-}) vibrations. In cerium(IV) sulfate hydrate, these bands typically appear in the asymmetric stretching (ν_3) around 1100 cm^{-1}, while the precipitated sample before calcination shows an intense absorption peak at around 1058.6 cm^{-1} corresponding to the symmetric (ν_1) stretching modes of sulfate anions respectively coordinated to Ce^{3+}, indicating well-defined Ce-OSO_3 linkages within the precursor matrix (Colthup et al., 1990). Two weak shoulders appeared around 1136.8 cm^{-1} and 993 cm^{-1} corresponded to the asymmetric (ν_3) and combination or overtone modes of the sulfate group or bending vibrations of hydroxylated sulfate species respectively (Colthup et al., 1990, Smith , 2011). These two peaks confirm the coexistence of oxyhydroxide and sulfate species after precipitation, suggesting that the treatment of cerium (IV) sulfate hydrate with ammoniuma hydroxide led to the formation of cerium hydroxide. Notably, the increased intensity and resolution of the IR bands following NH_4OH treatment indicate the formation of more well-defined chemical bonds, suggesting a fundamental rearrangement of the cerium compound's precursor structure. This structural modification correlates with the development of nanoporous particles observed via FESEM (Figure 3) and the enhanced crystallinity evidenced by XRD analysis (Figure 5).

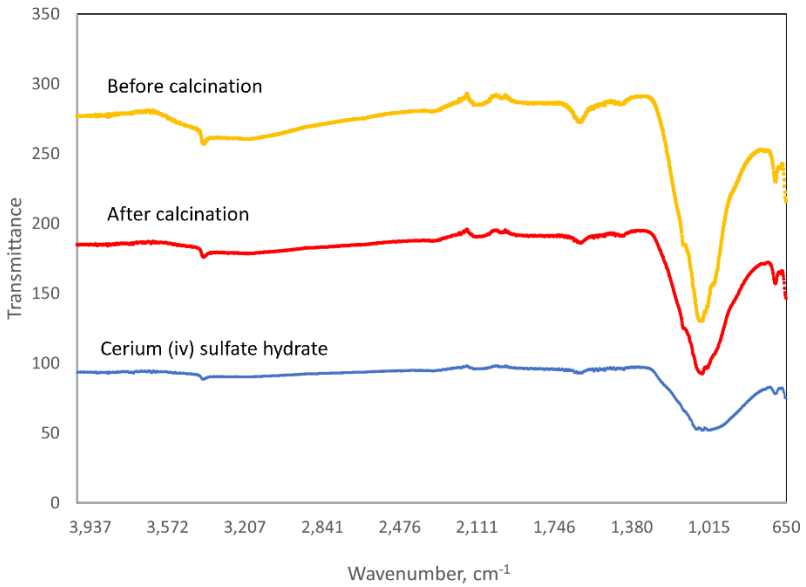

Figure 2: FTIR spectra of cerium sulfate (IV) hydrate as precursor, precipitate cerium suflate hydroxide before and after calcination

Following calcination at 600°C, significant changes were observed in the FTIR spectrum of the calcined sample (Figure 2). The broad O-H stretching band was substantially reduced, indicating dehydration of the material upon calcination. The disappearance of the sulfate bands at 993 cm^{-1}, confirms the successful removal of sulfate groups through thermal decomposition. The reduced intensity of other peaks between 1600 – 2800 cm^{-1} confirms minimal organic or carbonate contamination. The appearance of bands at 1643, 1555 and 1405 cm^{-1} referring to absorption of atmospheric carbon dioxide which nearly disappeared after calcination (Ramjeyanthi et al., 2019). A weak shoulder near 701 cm^{-1} can be attributed to Ce–O–H bending or lattice M–O vibrations, indicating the development of a metal–oxygen framework within the precursor (Colthup et al, 1990, Smith, 2011). According to Ramjeyanthi et al., 2019, absorption bands appearing below 800 cm^{-1} represents the metal-oxygen stretching (Ce-O stretch) which confirms the formation of CeO_2 particles. The presence of an intermediate-intensity spectrum suggests partial structural modification of the powder after calcination at 600 °C, while some characteristics of cerium sulfate are still retained.

Morphological Characterization

FE-SEM analysis in Figure 3 reveals distinct morphological differences among the precursor, the precipitate material before, and the calcined sample. The precursor shows irregular shape particles that are heavily agglomerated (Figure 3a) and exhibits a dense morphology (Figure 3b). In contrast, the precipitated cerium sulfate hydroxide displays more regularly shaped particles with reduced agglomeration (Figure 3c) and the presence of
porous structures on the particle surfaces (Figure 3d). Figure 3d and 3e compare the morphologies of the precipitated and post-calcination powders, respectively, demonstrating that calcination at 600 °C enhances the development of porosity. Figure 3f conforms that calcination transforms the precipitate into a nanoporous structure with a more uniform particle distribution. The size of the CeO_2 powders were in nano-range, however the specific size was not determined in this study.

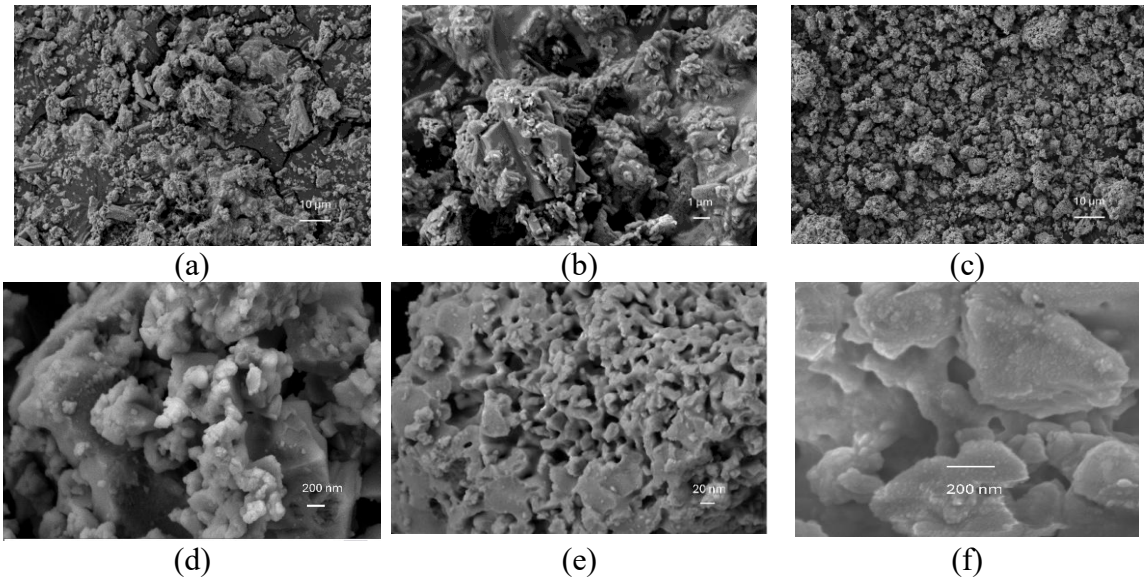

Figure 3: Surface morphology of cerium compound; (a) precursor shows irregular shape particles, (b) precursor exhibits dense structure, (c) precipitate has regular shape particles, (d) precipitate displays combination of dense and porous structure, (e) post-calcination precipitate has more obvious porous structure, (f) close-up image of uniform nano-sized CeO_2 powders with nanoporous structure after calcination.

Elemental analysis

Figure 4a shows the EDX spectrum for post-calcination precipitate, confirming that the powder contains only three elements which are Ce, O and S. Table 1 presents that the cerium content increases from 38.05 wt.% in the precursor to 64.3 wt.% in the post-calcination powder. Post-calcination analysis demonstrated that the sulfur was not eliminated completely, suggesting the crystallization process during precipitation is not sufficient. Longer ageing times may be required to enhance crystallization and promote further sulfur removal, and additional thermal treatment studies are necessary to evaluate the effectiveness of heat treatment in producing near–high-purity CeO_2.

Table 1: Elemental composition of precursor, precipitate before calcination and post-calcination.

Element	Samples / concentration (Wt.% ± Wt.% sigma)		
	CeSO4	Precipitate before calcination	Precipitate after calcination
Cerium (Ce)	38.05 (± 0.14)	55.29 (±0.26)	64.3 (±0.25)
Sulfur (S)	15.54 (± 0.07)	11.56 (±0.09)	10.75 (±0.12)
Oxygen (O)	46.41 (± 0.14)	33.16 (±0.20)	24.95 (±0.22)

Phase composition analysis

Figure 4 displays the XRD patterns of the precursor and the post-calcination precipitate. The patterns indicate the crystallinity of the post-calcination precipitate increases, confirming that the precursor is cerium (IV) sulfate hydrate, while the post calcined precipitate is CeO_2. The major diffraction peaks (2 theta) for CeO_2 could be indexed and lattice at 28.59° (111), 33.03° (200), 47.59° (220) and 56.36° (311), 69.62° (400) and 76.72° (331). The major diffraction peaks (2θ) for CeO_2 are observed at 28.59° (111), 33.03° (200), 47.59° (220), 56.36° (311), 69.62° (400), and 76.72° (331), consistent with previous reports (Malatesh et al., 2017). These results suggest that further thermal treatment may be necessary to enhance the crystallinity of CeO_2 and achieve a higher-purity product.

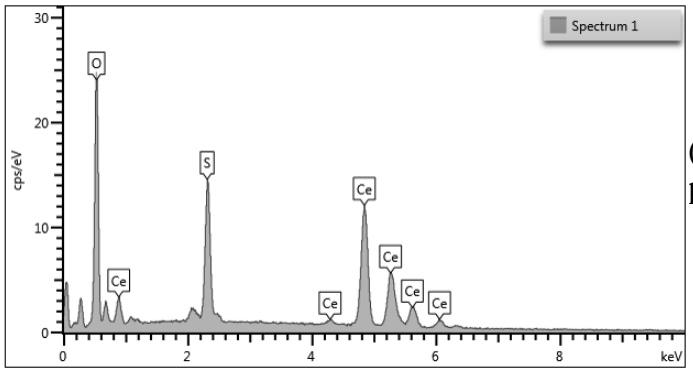

(a) EDS spectrum for post calcination powder

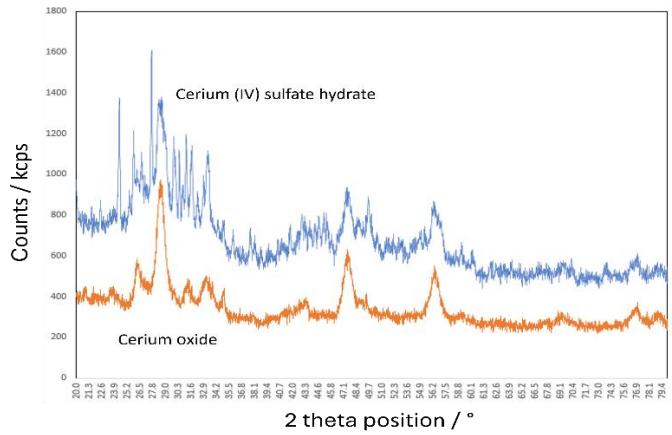

(b) XRD spectra for precursor, precipitate before and after calcining

Figure 4: (a) Elemental composition of the post-calcination powder, and (b) XRD patterns showing the phase composition of the precursor, precipitate before calcination, and post-calcination powder

Mass Balance and Yield Analysis

The yield of the precipitated powder, measured before and after calcination, indicated 85% mass retention following thermal treatment. The 15% mass loss is attributed to the removal of structural water and the decomposition of sulfate groups into volatile species (H_2O, SO_2, O_2). This observed yield consistent with the theoretical mass loss expected from the dehydration and desulfation reactions during calcination.

CONCLUSION

A simple and efficient precipitation-calcination method was successfully employed to synthesize CeO_2 from cerium (IV) sulfate hydrate. FTIR analysis confirmed the conversion of the hydroxide-sulfate precursor to CeO_2, evidenced by the disappearance of sulfate bands and emergence of characteristic Ce-O vibrations. FESEM-EDX analysis revealed the formation of nanoporous CeO_2 structures with uniform morphology and confirmed the elemental the purity of Ce, while XRD analysis confirmed the oxide phase formation and the crystallinity. The synthesis achieved 85% mass retention, demonstrating the efficiency of this route for CeO_2 production. The scalability and simplicity of this method make it attractive for industrial scale-production of high-quality CeO_2 nanoparticles. Future work will focus on optimizing calcination parameters to further improve yield and crystallinity, as well as evaluating the biosensing and catalytic performance of the synthesized CeO_2 nanoparticles to explore their practical applications.

REFERENCES

Alifanti, M., Baps B., Blangenois N., Naud J., Grange P., and Delmon B. (2003), Characterization of CeO2-ZrO2 Mixed oxides. Comparison of the citrate and sol-gel precipitation method. *Chemical Material*, 15 (2): 395. https://doi.org/10.1021/cm021274j

Bojana S, Zeljka A., Nadica A., Randeka K., Miodrag Mitric, Amelia M. and Miroslav D.D., (2008), Combustion synthesis and characterization of CeO2 Nanopowder, *Acta Chimica Slovenica*, 55: 486. https://vinar.vin.bg.ac.rs/handle/123456789/3545

Campbell, C. T. and Peden, C.H. F., (2005), Oxygen vacancies and catalysis on ceria surfaces. *Science*, 309 (5735): 713-714. https://doi.org/10.1126/science.1113955

Colthup, N.B., Daly, L.H. and Wiberley, S.E., (1990), Introduction to Infrared and Raman Spectroscopy (3rd ed.). Academic Press

Dahle, J. and Arai, Y., (2015), Environmental Geochemistry of Cerium: Applications and toxicology of cerium oxide nanoparticles. *International Journal of Environmental Research and Public Health*, 12 (2): 1253. https://doi.org/10.3390/ijerph120201253

Das, S., Dowding, J.M., Klump, K.E., McGinnis, J.F., Self, W. and Seal, S., (2013), Cerium oxide nanoparticles: Applications and prospects in nanomedicine, *Nanomedicine*, 3(3): 313. https://doi.org/10.2217/nnm.13.133

Gupta, C.K. and Krishnamurthy, N., (2005), Extractive Metallurgy of Rare Earths, CRC Press.

Krystof Skrbek and Ondrej Jankosvsky, (2019), Synthesis and characterization of ceria nanoparticles, *AiP Conference Proceedings,* 2170: 020018. https://doi.org/10.1063/1.5132737

Mahmoud A., Hussein, Ajahar Khan, and Khalid A. Alamry, (2022), A highly efficient electrochemical sensor containing polyaniline/cerium oxide nanocomposites for hydrogen peroxide detection. *RSC Advance*,12: 31506. https://doi.org/10.1039/D2RA05041B

Pujar, M.S., Hunagund, S.M., Desai, V.R, Patil, S. and Sidarai A. H., (2017), One-step synthesis and characterizations of cerium oxide nanoparticles in an ambient temperature via co-precipitation method. *AIP Conference Proceedings*, 1942: 050026-1. https://doi.org/10.1063/1.5028657

Phokha, S., Pinitsoontorn, S., Chirawatkul P., Poo-arporn Y. and Maensiri. S., (2012), Synthesis characterization and magnetic properties of monodisperse CeO2 nanospeheres prepared by PVP-assisted hydrothermal method. *Nanoscale Research Letters*, 7: 425. https://doi.org/10.1186/1556-276X-7-425

Pouretedal, H.R. and Kadkhodaie, A., (2010), Synthetic CeO2 nanoparticle catalysis of methylene blue photodegradation: kinetics and mechanism. *Chinese Journal of Catalyst*, 3 (11-12): 1328.
https://doi.org/10.1016/S1872-2067(10)60121-0

Ramjeyanthi, N., Alagar, M. and Muthuraman, D., (2019), Effect of calcination temperature on the structural and optical properties of Synthesised ceria nanoparticles via chemical method, *Journal of Applied Science and computations*, 5(9): 577.
ISSN Number: 1076-5131

Smith B.C., (2011), Fundamentals of Fourier Transform Infrared Spectroscopy (2nd ed.). CRC Press.

Sun, C., Li, H. and Chen, L., (2012), Nanostructured ceria-based materials: Synthesis, properties, and applications, *Energy & Environmental Science*, 5(9): 8475-8505.
https://doi.org/10.1039/C2EE22310D

Wang, H., Jian, M., Fan, J., He, Y. and Wang, Z., (2024), Scalable synthesis of Au@CeO_2 nanozyme for development of colorimetric lateral flow immunochromatographic assay, *Talanta*, 273: 125852.
https://doi.org/10.1016/j.talanta.2024.125852

Wang Y., Mori T., Li J. and Ikegami T., (2002), Lo temperature synthesis of praseodymium-ceria nanopowders. *Journal of American Ceramic Society*, 85: 3105.
https://doi.org/10.1111/j.1151.2916.2002.tb00591

Zhanxiao-Lu, Yarong Cheng, Zhang Y., Xuefeng Wang and Pengcheng Xu, (2021), Non-enzymatic free bilirubin electrochemical sensor based on ceria nanocube. *Sensors and Actuators: B. Chemical*, 329: 129224
https://doi.org/10.1016/j.snb.2020.2002.129224